

Cloud Cavitation Phenomena

C. Brennen, T. Colonius, Y.-C. Wang, A. Preston
 (California Institute of Technology, USA)

ABSTRACT

This paper describes investigations of the dynamics and acoustics of clouds of cavitation bubbles. Recent experimental and computational findings show that the collapse of clouds of cavitating bubbles can involve the formation of bubbly shock waves and that the focussing of these shock waves is responsible for the enhanced noise and damage in cloud cavitation. The recent experiments and computations of Reisman *et al.* (1) complement the work begun by Mørch and Kedrinskii and their co-workers (2,3,4) and demonstrate that the very large impulsive pressures generated in bubbly cloud cavitation are caused by shock waves generated by the collapse mechanics of the bubbly cavitating mixture. Here we describe computational investigations conducted to explore these and other phenomena in greater detail as part of an attempt to find ways of ameliorating the most destructive effects associated with cloud cavitation.

Understanding such bubbly flow and shock wave processes is important because these flow structures propagate the noise and produce the impulsive loads on nearby solid surfaces in a cavitating flow. How these shocks are formed and propagate in the much more complex cloud geometry associated with cavitating foils, propeller or pump blades is presently not clear. However, the computational investigations reveal some specific mechanisms which may be active in the dynamics and acoustics of these more complex flows.

1. NOMENCLATURE

a Amplitude of plate motion

A Radius of the bubble cloud
 A_0 Initial radius of the bubble cloud
 C_p Pressure coefficient, $(p - p_0)/\frac{1}{2}\rho U^2$
 C_{pmin} Minimum pressure coefficient
 D Reference body size
 k Polytropic constant for gas inside the bubble
 p Fluid pressure (Pa)
 p_0 Upstream reference pressure (Pa)
 p_v Vapor pressure
 R Bubble radius
 R_0 Initial radius of the bubble
 t Time
 T Period of plate oscillation
 U Reference velocity of the flow (m/s)
 α Void fraction of the bubbly mixture
 α_0 Initial void fraction of bubbly mixture
 α_c Critical void fraction
 β Cloud interaction parameter, $\alpha_0 A_0^2 / R_0^2$
 ρ Density of the liquid
 σ Cavitation number, $(p_0 - p_v)/\frac{1}{2}\rho U^2$

2. INTRODUCTION

In many flows of practical interest, clouds of cavitation bubbles are periodically formed and then collapse. This temporal periodicity may occur naturally as a result of the shedding of bubble-filled vortices or it may be the response to a periodic disturbance imposed on the flow. Common examples of imposed fluctuations are the interaction between rotor and stator blades in a pump or turbine and the interaction between a ship's propeller and the non-uniform wake created by the hull. When the density of cavitation events increases in space or time and bubbles therefore begin to interact, a whole new set of phenomena may be manifest

both in the dynamics and the acoustics. In many of these cases the coherent collapse of the cloud of bubbles can cause a substantial increase in the radiated noise and potential for damage. Much recent interest has focused on the dynamics and acoustics of finite clouds of cavitation bubbles because of these very destructive effects (see, for example, Knapp (5), Bark and van Berlekom (6), Soyama *et al.* (7)). The purpose of the computational investigations outlined in this paper is to explore the various phenomena which can occur in the dynamics and acoustics of these bubbly cavitating flow and, where possible, to compare these with experimental observations.

1. Some Recent Experiments on Cloud Cavitation

Numerous investigators (for example, Knapp (5), Wade and Acosta (8), Bark and van Berlekom (6), Shen and Peterson (9,10), Bark (11), Franc and Michel (12), Hart *et al.* (13), Kubota *et al.* (14,15), Le *et al.* (16), de Lange *et al.* (17), Kawanami *et al.* (18)) have studied the complicated flow patterns involved in the production and collapse of cloud cavitation on a hydrofoil. The basic features of the cyclic process of cloud formation and collapse (whether on a stationary or oscillating foil) are as follows. The growth phase usually involves the expansion of a single attached cavity, at the end of which a re-entrant jet penetrates the cavity from the closure region. This penetration breaks the cavity into a bubbly cloud which collapses as it is convected downstream.

The radiated noise all occurs during this bubbly part of the cycle. It consists of pressure pulses of very short duration and large magnitude. The pulses have been observed and measured by a number of investigators including Bark (11), Bark and van Berlekom (6), Le *et al.* (16), Shen and Peterson (9,10), McKenney and Brennen (19) and Reisman *et al.* (20). More recently, Reisman *et al.* (1) have made measurements of the impulsive pressures on the suction surface of a hydrofoil (within the cloud cavitation), have simultaneously measured the radiated pulses and have correlated these pressure traces with images from high-speed movies. Very large pressure pulses were recorded by the surface transducers, with typical magnitudes as large as 10bar and durations of the order of 10^{-4} s. These help to explain the enhanced noise and cavitation damage associated with cloud cavitation. For example, the large impulsive surface loadings due to

these pulses could be responsible for the foil damage reported by Morgan (21), who observed propeller blade trailing edges bent away from the suction surface and toward the pressure surface.

Reisman *et al.* (1) also correlated high-speed movies of the clouds with the pressure measurements and found that the pressure pulses recorded (both on the foil surface and in the far field) were associated with specific structures (more precisely, the dynamics of specific structures) which are visible in the movies. Indeed, it appears that several types of propagating structures (shock waves) are formed in a collapsing cloud and dictate the dynamics and acoustics of collapse. One type of shock wave structure is associated with the coherent collapse of a well-defined bubble cloud which separates from the rear of the cavitation zone and is convected downstream. This type of structure causes the largest impulsive pressures and radiated noise. The pulses it produces are termed *global* pulses since they are recorded almost simultaneously by all transducers. The high-speed motion pictures showed that the cavitation cloud undergoes a rapid and coherent collapse and that these collapses generate the global pulses. It was noted that such cloud collapses do not involve large and rapid changes in the volume of the cloud. Rather, they involve rapid and propagating changes in the void fraction distribution within the cloud.

Unexpectedly, two other types of structures were observed. Typically, the pulses produced by these structures were registered by only one transducer and these events were therefore termed *local* pulses. They are recorded when an ephemeral, localized and transient low void fraction structure forms in the bubbly cavitating cloud and happens to pass over the face of the transducer. While these *local* events are smaller and therefore produce less radiated noise, the pressure pulse magnitudes are almost as large as those produced by the *global* events. How and why these low void fraction structures (shock waves) form in the flow is not at all clear.

Finally, we note that injection of air into the cavitation on the suction surface can substantially reduce the magnitude of the pressure pulses produced (Ukon (22), Arndt *et al.* (23), Reisman *et al.* (24)). However Reisman *et al.* (25) have shown that the bubbly shock wave structures still occur; but with the additional air content in the bubbles, the pressure pulse magnitudes are greatly reduced.

2. On Calculations of Cloud Cavitation

The experimental and practical observations of cloud cavitation exemplified by the preceding discussion have generated much interest in modelling the dynamics and acoustics of these flows. These efforts began with the work of van Wijngaarden (26) who first attempted to model the behavior of a collapsing layer of bubbly fluid next to a solid wall. The essence of his approach was to couple conventional continuity and momentum equations for the compressible mixture to a Rayleigh-Plesset equation for the bubble dynamics (see, for example, Brennen (27)) which would provide the necessary relation connecting the local pressure with the bubble size and therefore the local mixture density. This is the basis for most of the computational investigations which have been carried out subsequently. Later investigators explored numerical methods which incorporate the individual bubbles (Chahine (28)) and continuum models which, for example, analyzed the behavior of shock waves in a bubbly liquid (Noordzij and van Wijngaarden (29), Kameda and Matsumoto (30)) and identified the natural frequencies of spherical clouds of bubbles (d'Agostino and Brennen (31)). Indeed the literature on the linearized dynamics of clouds of bubbles has grown rapidly (see, for example, d'Agostino *et al.* (32,33), Omta (34), Prosperetti (35)). However, apart from some weakly non-linear analyses (Kumar and Brennen (36,37,38)) only a few papers have addressed the highly non-linear processes which are an inevitable consequence of the non-linearities in the Rayleigh-Plesset equation and are most evident during the collapse of a cloud of bubbles. Chahine and Duraiswami (39) have conducted numerical simulations using a number of discrete bubbles and demonstrated how the bubbles on the periphery of the cloud develop inwardly directed re-entrant jets. However, most clouds contain many thousands of bubbles and it therefore is advantageous to examine the non-linear behavior of continuum models.

Another perspective on the subject of collapsing clouds was that introduced by Mørch and Kedrinskii and their co-workers (Mørch (2,3), Hanson *et al.* (4)). They surmised that the collapse of a cloud of bubbles involves the formation and inward propagation of a shock wave and that the geometric focusing of this shock at the center of cloud creates the enhancement of the noise and damage potential associated with cloud collapse. We begin the re-

view of computational efforts by describing studies of the dynamics of a spherical cloud of bubbles, a simple example which illustrates these processes of shock wave formation, propagation and focussing.

3. Computations: [1] Dynamics of a Spherical Cloud

Wang and Brennen (40,41,42) (see also Reisman *et al.* (1)) used a mixture model comprising the continuity, momentum and Rayleigh-Plesset equations (for specifics see, for example, d'Agostino *et al.* (31,32,33)) to study the non-linear growth and collapse of a spherical cloud of bubbles. A finite cloud of nuclei is subjected to an episode of low pressure which causes the cloud to cavitate; the pressure then returns to the original level causing the cloud to collapse. Wang and Brennen used the computational model to study the various cloud dynamics and acoustics exhibited in various parametric regimes. Key parameters are the cavitation number, σ , which characterizes the the initial pressure level, the magnitude of the low pressure episode characterized by a minimum pressure coefficient, C_{pmin} , and by a duration, D/U . The initial radius and void fraction of the cloud are denoted by A_0 and α_0 respectively and the initial radius of the bubbles within the cloud is denoted by R_0 .

This parametric exploration revealed that the dynamics and acoustics depended in an important way on the "cloud interaction parameter", β , defined as

$$\beta = \alpha_0 A_0^2 / R_0^2 \quad (1)$$

Note that, while the initial void fraction, α_0 , is very small, the ratio, A_0/R_0 , may be very large so that β could be small or large compared with unity. Earlier linear and weakly nonlinear studies of cloud dynamics (d'Agostino & Brennen (31,32,33), Kumar & Brennen (36,37,38)) showed that the cloud natural frequency is strongly dependent on this parameter. If β is small, the natural frequency of the cloud is close to that of the individual bubbles in the cloud. In other words, the bubbles in the cloud tend to behave as individual units in an infinite fluid and the bubble/bubble interaction effects are minor. On the other hand bubble interaction effects dominate when the value of β is greater than order one. Then the collective oscillation of bubbles in the cloud results in a cloud natural frequency which is lower than the natural frequency of individual bubbles.

In all of the computations of Wang and Bren-

nen, the bubbles in the interior of the cloud are shielded by the outer shell of bubbles and grow to a smaller maximum size. This shielding effect is typical of the bubble/bubble interaction phenomenon in cavitating cloud dynamics (d'Agostino & Brennen (31,33); Ornta (34); Smereka & Banerjee (48); Chahine & Duraiswami (39)).

The non-linear computations showed that when $\beta \gg 1$, spherical cloud collapse began on the cloud surface and propagated inwards as a collapse front. As a result of the bubble collapse within this front, a large pressure pulse or shock wave becomes an integral part of the propagating collapse front. The structure of this shock is very similar to those in the bubbly flows investigated by Noordij and van Wijngaarden (29) and other investigators (see, for example, Brennen (27), Kameda and Matsumoto (30)); the shock is comprised of a series of rebounds and secondary collapses. The locations with small bubble size represent regions of low void fraction and higher pressure due to the local bubble collapse. The magnitude of the pressure pulse grows due to geometric focussing as the front progresses inward and reaches very large magnitudes when it reaches the center of the cloud. At this instant a very large, positive pressure pulse is radiated away from the cloud into the far-field; all the earlier or later radiated noise is almost insignificant by comparison. Another characteristic of the collapse is the relatively small change which occurs in the cloud radius, A . The essential collapse process is unlike that of a single bubble and involves the propagation of void fraction waves within the cloud rather than radical volumetric change.

In contrast, Wang and Brennen found that the dynamics and acoustics when $\beta \ll 1$ were quite different. Then collapse began with the bubbles at the cloud center and the collapse front propagated outward producing a much more benign process and much reduced radiated noise.

[Parenthetically we note that all of the preceding computations were done with a cloud consisting of a uniform dispersion of identical bubbles. Real clouds will have a distribution of bubble sizes. Wang (43) has recently developed a computational methodology to deal with this more complex circumstance. Moreover, he observes some significant differences in the dynamics and acoustics of these non-monodisperse clouds.]

When compared with the experimental observations of Reisman *et al.* (1) and others, the results

of the computations of Wang and Brennen reveal many parallels. First note that the value of β in a real flow will increase as the cavitation number is decreased and more and more nuclei are activated. Thus the critical value of β of about unity may be manifest in practice as a critical cavitation number below which cloud cavitation begins.

Secondly, we note that shock waves characterized by large, positive pressure pulses and zones of low void fraction may form during the cloud collapse process. They will then propagate through the cloud and can grow to very large magnitudes due to geometric focussing. Such structures were observed by Reisman *et al.*(1).

Finally we note that there may be important implications for model testing in water tunnels. Since α_0 and R_0 tend to be similar at the model and full scales but A_0 could be radically different, it follows that the model tests might be conducted at much smaller values of β than pertain at full scale. Consequently there is a real risk that violent cloud cavitation could occur at full scale and not at the model scale.

4. Computations: [2] Harmonic Cascading

We now shift attention to a different set of computational investigations in order to discuss two other non-linear acoustic phenomena which have been identified from the calculations of cloud dynamics. Both of these emerge from calculations of the response of a liquid layer (laced with cavitation nuclei or bubbles but at small void fraction) to the vibration of an infinite flat plate in a direction normal to its surface. Kumar and Brennen (36,38) present both the linear and a weakly non-linear solution to this problem utilizing the same set of model equations described above. While a multitude of non-linear effects occur in the weakly non-linear solution (in which terms quadratic in the oscillation amplitude are retained but all higher order terms are neglected) we highlight just one here because of its practical significance. This emerges from calculations using typical size distributions of bubbles; each size, of course, has its own single bubble natural frequency with the larger number of smaller bubbles having a much higher natural frequency than the fewer, larger bubbles.

Kumar and Brennen (37) identify a phenomenon they call *harmonic cascading*. In this process the larger bubbles, responding mostly to oscillations

at their relatively low natural frequency, produce higher harmonics due to non-linear effects. These higher frequencies in turn excite a much larger number of smaller bubbles because that higher harmonic corresponds to the basic natural frequency of those smaller bubbles. The measured spectra of cavitation reported by Mellen (44) and by Blake *et al.* (45) contain peaks which may well be due to *harmonic cascading*. In any case, it seems clear that non-linear effects combined with a typical bubble number distribution provide a mechanism for the cascading of acoustic energy from low frequencies to high frequencies where the attenuation is, in turn, more effective in damping the noise.

5. Computations: [3] Acoustic Saturation

A second notable phenomenon emerges from fully non-linear calculations of the same physical problem of a liquid layer and will be referred to as *acoustic saturation*. In this case a distribution of bubble sizes is not essential and so results are presented for nuclei of just one uniform equilibrium size. Colonius *et al.* (46) and Brennen *et al.* (47) demonstrate what happens as the amplitude of the plate oscillation is increased from the linear regime up to the highly non-linear regime in which true cavitation bubble collapse occur. The bubbles next to the wall behave as expected as the amplitude is increased as illustrated in figure 1. This shows the typical development of a Rayleigh-Plesset solution with increasing amplitude. We note that in this and the other results presented in this section, that the bubble damping has been adjusted to a value which is consistent with the experimentally observed spatial attenuation of acoustic waves in bubbly liquids. This also produces a more realistic number of rebounds than the much smaller value used in the nozzle calculations of the next section (see Colonius *et al.* (46)).

More unexpected is the behaviour of the bubbles further away from the plate. At low amplitudes the sinusoidal pressure oscillations produced by the oscillating plate simply propagate away with an amplitude directly proportional to the amplitude of motion of the plate. But, as non-linear effects begin to become significant, the radiated signal is attenuated relative to the expected linear magnitude and, eventually, reaches an asymptotic value. This phenomenon is illustrated in figures 2, 3 and 5. Figure 2 presents the typical pressure signals occurring at a distance from the plate and the

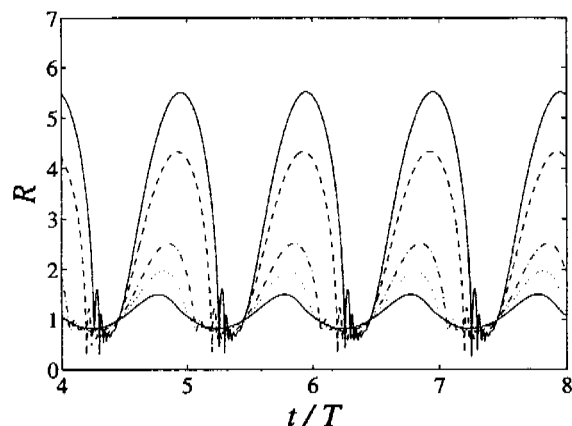


Figure 1. Typical radii/time histories for the bubbles at the surface of the plate for plate velocity amplitudes, a , equal to 0.05 (solid line), 0.075 (dots), 0.1 (dash-dot), 0.2 (dashes) and 0.3 (solid line). The initial void fraction and cavitation number are respectively 0.01 and 0.475 and other parameters are given in Colonius *et al.* (46).

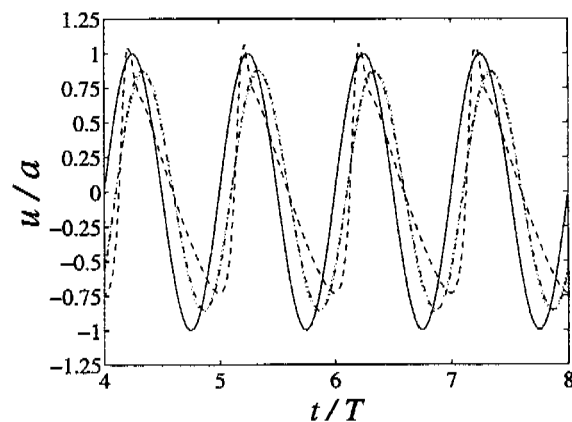


Figure 2. The fluid velocity (*normalized by the velocity amplitude at the plate surface*) at the plate surface (solid line) and at a distance of 400 initial bubble radii into the fluid as a function of reduced time for plate velocity amplitudes, a , equal to 0.0001 (dots), 0.001 (dash-dot) and 0.01 (dashes) initial bubble radii. The initial void fraction and cavitation number are respectively 0.01 and 0.475 and other parameters are given in Colonius *et al.* (46).

essentially linear behavior at low amplitudes (the vertical coordinate is the instantaneous fluid velocity *normalized by the magnitude of the wall velocity oscillations*). On the other hand, figure 3 presents the typical behaviour at large amplitudes; the *non-normalized* signals at a distance from the plate are almost independent of the plate amplitude. Thus further increase in the plate oscillation amplitude produces no change in the radiated noise. This

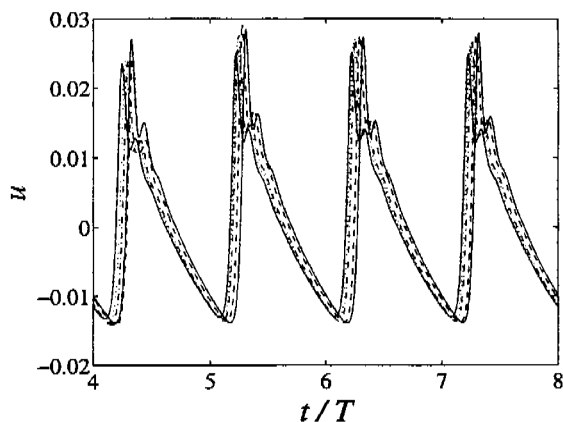


Figure 3. As figure 2 but larger amplitude plate motions, a ; equal to 0.05 (solid line), 0.075 (dots), 0.1 (dash-dot), 0.2 (dashes) and 0.3 (solid line) initial bubble radii. Note that, unlike figure 2, the vertical scale is not normalized by a . From Colonius *et al.* (46).

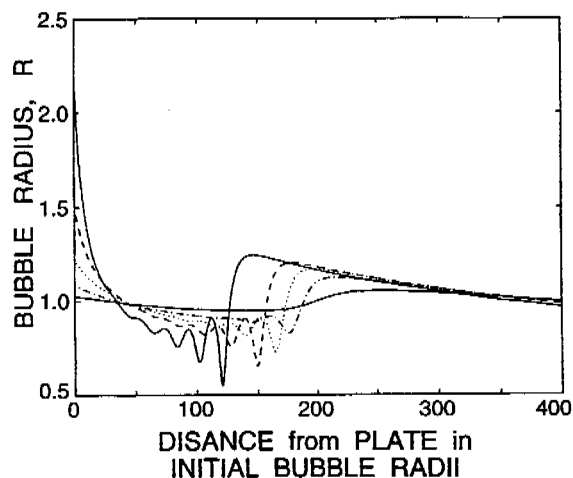


Figure 4. Snapshots at one moment in time ($t/T = 76$) of the variation in bubble radius with distance from the plate for the same case as figure 1.

is, in part, caused by the formation of a highly active layer adjacent to the plate where the bubbles grow large enough that their momentary natural frequency is no longer large compared to the plate oscillation frequency. Thus acoustic energy is trapped and dissipated in this layer near the plate (see also Smereka and Banerjee (48)). Increasing the plate amplitude simply results in greater dissipation and in no increase in the radiated noise. The nature of the layer for this particular case is further illustrated in figure 4. Note that the layer decreases in thickness from about 200 initial bubble radii at an amplitude of $a = 0.025$ to 120 initial bubble radii at $a = 0.3$. The figure clearly shows how the response increases with amplitude within the layer but is independent of amplitude outside the layer.

The acoustic saturation phenomenon in this case is summarized in figure 5 which plots the magnitude of the bubble radius oscillations some distance from the plate as a function of the amplitude of the plate oscillations. This clearly demonstrates the *acoustic saturation* phenomenon. It could be a contributing factor to the frequently made experimental observation that, as the pressure in a flow is decreased and the cavitation increases, the noise often plateaus out and may even decrease after a certain point.

Finally, we remark that the description of the acoustic saturation phenomenon given above is pertinent to the sub-resonant behaviour manifest when the plate oscillation frequency is substan-

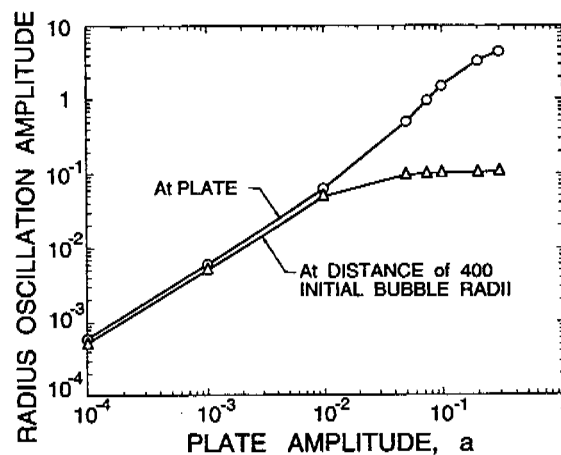


Figure 5. The amplitude of the bubble radius oscillations for the computations of figures 2 and 3 as a function of the plate amplitude, a . The circles are the bubble radius amplitudes at the wall and the crosses are the bubble radius amplitudes at a distance from the wall of 400 initial bubble radii.

tially smaller than the natural frequency of the individual bubbles in the fluid. Other non-linear effects are exhibited when the plate frequency approaches or exceeds the bubble natural frequency. Then, as anticipated by Smereka and Banerjee (48) (see also Lauterborn and Koch (49)) and confirmed by Brennen *et al.* (47), the non-linear effects produce a cascade of bifurcations leading, eventually, to a chaotic response of the bubbly fluid. This super-resonant regime is not, however, of great practical interest for, other than in the context of ultrasonic cavitation, it is uncommon to en-

counter circumstances in which the imposed excitation reaches such a high frequency.

6. Computations: [4] Steady Flow through a Nozzle

All of the above computations involve bubbly liquids which are not flowing in the mean. It is more challenging to devise numerical methodologies for cases in which the bubbly liquid is flowing and particularly difficult when dealing with a two- or three-dimensional flow. In this section we examine a case of a one-dimensional cavitating flow, namely that through a nozzle. When the same approach is applied to such a bubbly cavitating flow the solutions exhibit several interesting features which may provide insight into more complex two and three dimensional flows such as those over hydrofoils or propeller blades. Using the same basic equations previously discussed, namely a continuity equation, an inviscid momentum equation and the Rayleigh-Plesset equation to connect the local pressure with the local mixture density or bubble size, Wang and Brennen (50) present results for the one-dimensional, bubbly, frictionless cavitating flow through a convergent/divergent nozzle. The following typical flow will illustrate the phenomena manifest in the nozzle computations. A bubbly liquid, composed of air bubbles ($k = 1.4$) in water at 20°C (liquid density, 1000 kg/m, surface tension, 0.073 N/m), flows through a nozzle whose total length is 500 initial upstream bubble radii. The minimum or throat pressure coefficient for incompressible flow is -1.0 and the present example is for an upstream cavitation number, σ , of 0.8. The Reynolds number is also important since it determines the damping of the bubble oscillations (see Wang and Brennen (50)). It could be chosen, as suggested by Chapman and Plesset (51), so as to accommodate other, non-viscous contributions to the bubble damping. Five different upstream void fractions, α_0 , of the order of 10^{-6} are used in the computation and the results are shown in figures 6, 7, 8 and 9. Figures 6 and 7 respectively present the axial variations of the mixture velocity and the mixture pressure coefficient in this typical calculation.

The case of $\alpha_0 = 0$ corresponds to the incompressible pure liquid flow. It is notable that even for an upstream void fraction as small as 2×10^{-6} , the characteristics of the flow are radically changed from the case without bubbles. Radial pulsation of bubbles results in the downstream fluctuations of

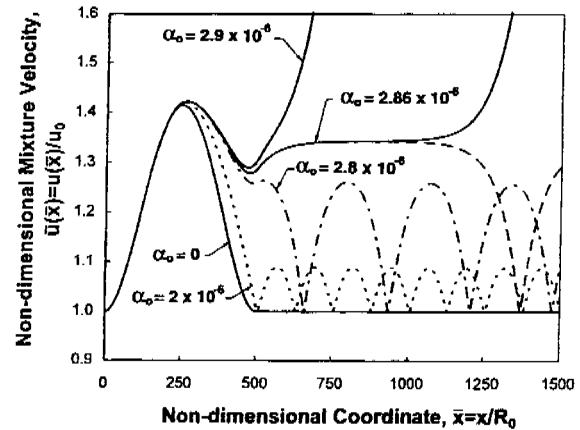


Figure 6. The non-dimensional mixture velocity distribution in the flow for five different upstream void fractions, α_0 , from Wang and Brennen (50). The dimensionless length of the nozzle is 500 with the throat located at 250; the cavitation number, $\sigma = 0.8$, the throat pressure coefficient for incompressible flow is -1.0 and other parameters are as given in the original reference. Note that, for this case, the critical value of the void fraction is 2.862×10^{-6} .

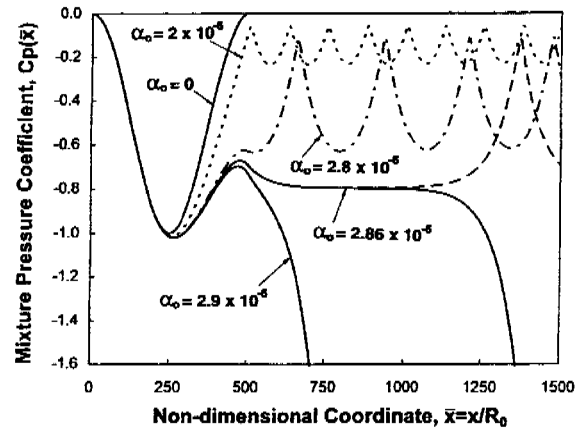


Figure 7. The mixture pressure coefficient corresponding to figure 6. From Wang and Brennen (50).

the flow. The amplitude of the velocity fluctuation is 10% of that of the incompressible flow in this case. As α_0 increases further, the amplitude as well as the wavelength of the fluctuations increase. However, the velocity does eventually return to the upstream value. In other words, the flow is still “quasi-statically stable.” However, as α_0 increases to a critical value, α_c ($\alpha_c \approx 2.862 \times 10^{-6}$ in the present example), a bifurcation occurs. Wang and Brennen (50) show that a critical state is reached downstream of the nozzle when the instantaneous bubble radius, R_c , reaches a value given approxi-

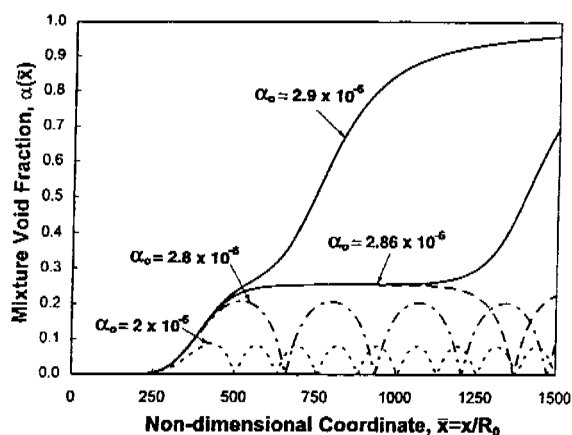


Figure 8. The void fraction distribution corresponding to figure 6. From Wang and Brennen (50).

mately by

$$R_c \approx R_0 \left[\frac{\sigma}{2\alpha_0(1-\alpha_0)} \right]^{1/3} \approx R_0 \left[\frac{\sigma}{2\alpha_0} \right]^{1/3} \quad (2)$$

where R_0 is the radius of the bubbles (assumed monodisperse) in the upstream flow. This implies that when the instantaneous bubble size exceeds R_c , the flow becomes unstable and flashes. In the context of an experiment in which only the upstream void fraction, α_0 , is increased while the other parameters are held fixed, this implies that the flow will flash at a critical value of the upstream void fraction, α_c , which in the present example yields $(\sigma/2\alpha_c)^{1/3} \approx 51$. Figure 9 demonstrates the veracity of the above expression for R_c/R_0 .

The flow becomes quasi-statically unstable and flashes to vapor if the radius of the cavitating bubbles is greater than R_c . In this circumstance, the growth of bubbles increases the mixture velocity due to mass conservation of the flow. The velocity increase then causes the mixture pressure to decrease according to the momentum equation. The decrease of the pressure is fed back to the Rayleigh-Plesset equation and results in further bubble growth. In this case the velocity and void fraction of the mixture increase and the pressure coefficient of the flow decreases significantly below the upstream values and the flow flashes to vapor. On the other hand, if the bubbles do not grow beyond R_c , the flow is quasi-statically stable and is characterized by large amplitude spatial fluctuations downstream of the throat.

Figure 8 illustrates the void fraction distribution in the flow. When the flow becomes quasi-statically unstable, the bubble void fraction quickly

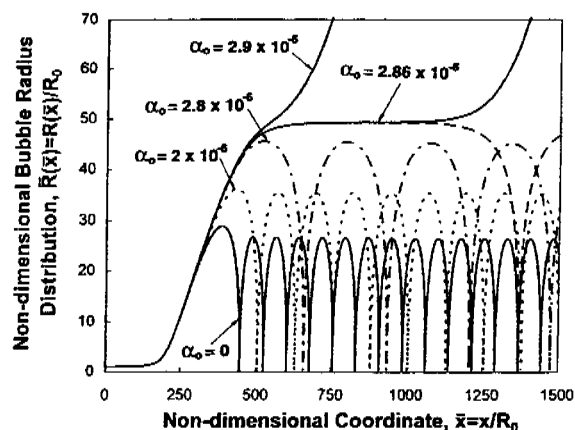


Figure 9. The non-dimensional bubble radius distribution corresponding to figure 6. From Wang and Brennen (50).

approaches unity. This means that the flow is flashing to vapor. However, it should be cautioned that when α becomes large, the present model loses validity since it is limited to flows with small void fraction. Figure 9 indicates the non-dimensional bubble radius distribution in the flow. Due to time lag during the bubble growth phase, bubbles reach the maximum size downstream of the throat. With increase in the upstream void fraction, the maximum size of the bubbles increases and is shifted further downstream. The bubbles grow without bound after reaching a critical radius, R_c , at which flashing begins.

Note from figure 7, that the downstream mixture pressure does not return to the upstream value except in the case of the pure liquid flow. Since viscous effects are neglected in the global mixture flow and the only dissipation present is that in the Rayleigh-Plesset equation representing bubble dynamic damping, the pressure and energy losses are caused by the radial motion of bubbles and are therefore "cavitation losses."

In addition to the two different flow regimes, another important feature in the quasi-statically stable flow is the typical frequency associated with the downstream periodicity. This "ringing" will result in acoustic radiation at frequencies corresponding to this wavelength. How this ring frequency relates to the upstream flow condition remains to be studied.

In summary, it is found that the nonlinear bubble dynamics coupled with the equations of motion of the mixture strongly affect the structure of the

flow even for very small bubble populations. Two different flow regimes, distinguished by the parameter $R_c = R_0(\sigma/2\alpha_c)^{1/3}$, are revealed in the steady state solutions. The results also imply that there exists a domain of pressure drops and void fractions for which no steady state flow solution exists. It remains to be determined whether those conditions lead to the unsteady, oscillatory cavitating flows which are observed in practice.

7. Computations: [5] Two and Three-dimensional Cavitating Bubbly Flows

It is more challenging to devise numerical methodologies for two and three-dimensional bubbly cavitating flows. In this regard we should mention several recent efforts to develop approximate methods for two-dimensional flows. Both Song (52) and Merkle and Feng (53) have modified compressible gas dynamic codes, introducing some artificial algebraic equation of state to relate the mixture density to the pressure. While these results are of some qualitative value they omit the essential bubble dynamic effects which would result from a more appropriate differential "equation of state" such as implied by the Rayleigh-Plesset equation. Perhaps Kubota *et al.* (15) come closest to a true two-dimensional methodology; however, by not permitting the bubbles to collapse below the original nuclei size, they exclude the formation of the large pressure perturbations and shock waves which are such an important part of cloud cavitation.

8. Computations: [5] Example: Encounter of Low Pressure Pulse with a Cylindrical Cloud

We illustrate some of the multidimensional phenomena by presenting preliminary computational results for a particularly simple two-dimensional calculation, namely the response of a cylindrical bubble cloud to an incident, planar pressure pulse (specifically a low pressure pulse) travelling through the liquid (which is assigned some compressibility so the progress of the wave may be recorded). The initial conditions are shown in figure 10. In this particular example the initial bubble cloud has a Gaussian radial distribution of void fraction reaching a maximum of 0.5% at the center of the cloud. The gray scale of the right-hand image depicts the void fraction distribution while that in the left-hand image shows the liquid density and, by implication, the pressure and scattered waves.

The incident wave moves from left to right in the sequence of images, figures 10 through 15, and is diffracted and scattered by the low sound speed inside the cloud. The pressure in the wave is low enough to cause cavitation and the bubbles within the cloud grow to nearly 100 times their original volume before collapsing violently. The bubbles on the left-hand side of the cloud grow first and collapse first, the latter process initiating a collapse front which propagates from left to right through the cloud. Sufficient damping is included in the Rayleigh-Plesset equation so that only a few bubble rebounds occur, but these are evident in the scattered sound (see figure 15).

9. Concluding Comments

In this paper we have summarized some of the recent advances in our understanding of bubbly cloud cavitation. It is becoming clear that effects of the interaction between bubbles may be crucially important especially when they give rise to the phenomenon called cloud cavitation. Calculations of the growth and collapse of a spherical cloud of cavitating bubbles show that when the cloud interaction parameter (β) is large enough, collapse occurs first on the surface of the cloud. The inward propagating collapse front becomes a bubbly shock wave which grows in magnitude due to geometric focussing. Very large pressures and radiated impulses occur when the shock reaches the center of the cloud.

Of course, actual clouds are far from spherical. And, even in a homogeneous medium, gasdynamic shock focussing can be quite complex and involves significant non-linear effects (see, for example, Sturtevant and Kulkarny (54)). Nevertheless, it seems evident that once collapse is initiated on the surface of a cloud, the propagating shock will focus and produce large local pressure pulses and radiated acoustic pulses. It is not, however, clear exactly what form the foci might take in the highly non-uniform, three-dimensional bubbly environment of a cavitation cloud on a hydrofoil, for example.

Experiments with hydrofoils experiencing cloud cavitation have shown that very large pressure pulses occur within the cloud and are radiated away from it during the collapse process. Within the cloud, these pulses can have magnitudes as large as 10bar and durations of the order of $10^{-4}s$. This suggests a new perspective on cavitation damage and noise in flows which involve large collec-

Figures 9 through 15. A series of snapshots in time of a planar pressure pulse impinging on a cylindrical cloud. The image on the left shows the fluid density (the white circle is the initial location of the cloud) while that on the right shows the void fraction distribution. Note that the image on the right is a close-up view compared with that on the left.

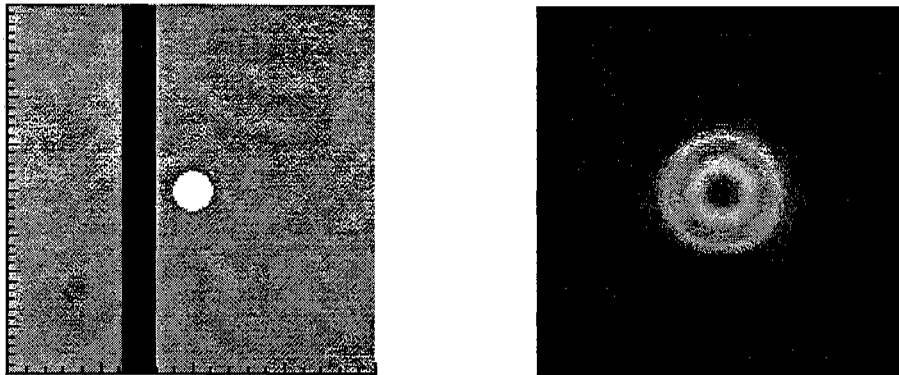


Figure 10. Initial conditions with low pressure pulse (vertical) moving from left to right and about to impinge on the cylindrical bubble cloud.

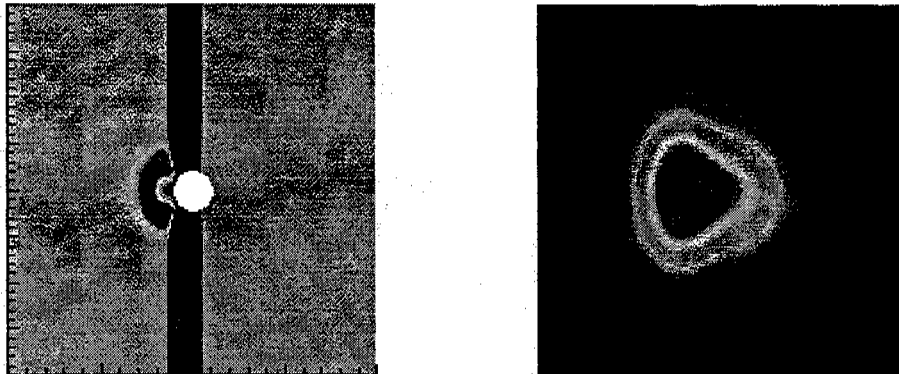


Figure 11. Expansion (or cavitation) of cloud.

tions of cavitation bubbles with a sufficiently large void fraction (or, more specifically, a large enough β) so that the bubbles interact and collapse coherently. This view maintains that the cavitation noise and damage is generated by the formation and propagation of bubbly shock waves within the collapsing cloud. The experiments reveal several specific shock wave structures. One of these is the mechanism by which the large coherent collapse of a finite cloud of bubbles occurs. A more unexpected result was the discovery of more localized bubbly shock waves propagating within the bubbly mixture in several forms, as crescent-shaped regions and as leading edge structures. These seem to occur when the behavior of the cloud is less coherent. They produce surface loadings which are

within an order of magnitude of the more coherent events and could also be responsible for cavitation damage. However, because they are more localized, the radiated noise they produce is much smaller than that due to global events.

The phenomena described are expected to be important features in a wide range of cavitating flows. However, the analytical results clearly suggest that the phenomena may depend strongly on the cloud interaction parameter, β . If this is the case, some very important scaling effects may occur. It is relatively easy to envision a situation in which the β value for some small scale model experiments is too small for cloud effects to be important but in which the prototype would be operating at a much larger β due to the larger cloud size, A_0 (assuming the

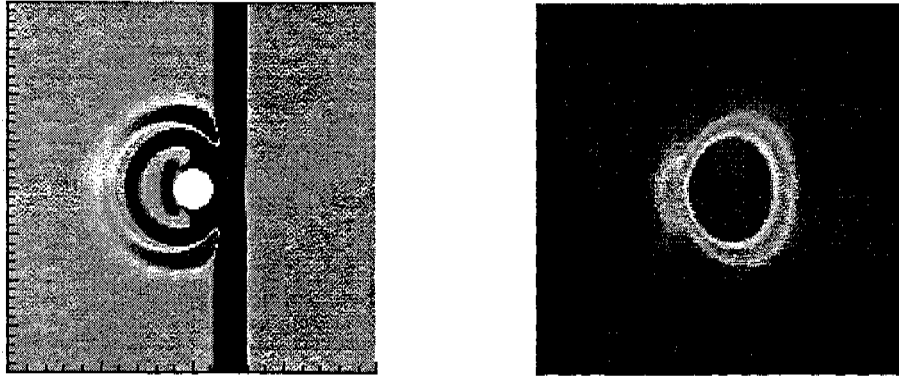


Figure 12. Scattered wave. Collapse beginning on left side of cloud.

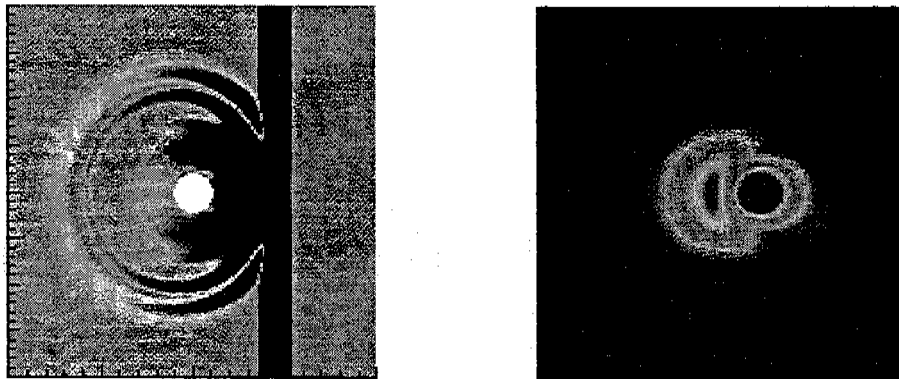


Figure 13. Collapse front moves through cloud from left to right.



Figure 14. Collapse produces second radiated pulse.

void fractions and bubble sizes are comparable). Under these circumstances, the model would not manifest the large cloud cavitation effects which could occur in the prototype.

Computational methods will play a key role in

these developing studies. Not only will such methods be needed for the prediction of these flows in practical applications (particularly to predict the noise and damage potential) but they are almost essential in building our understanding of simpler

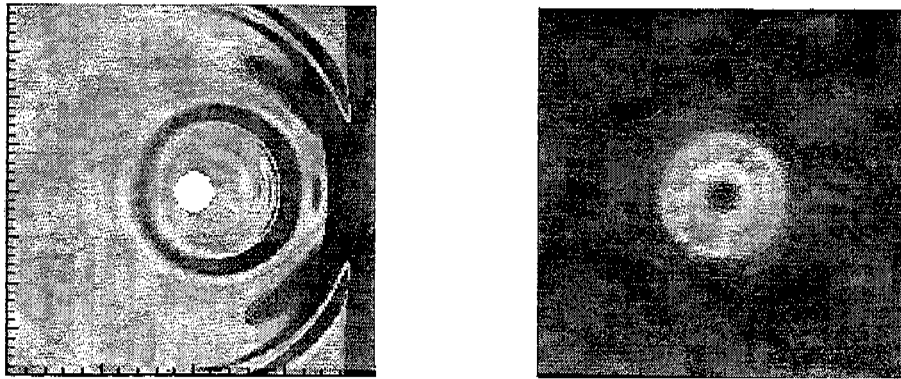


Figure 15. Cloud returning to original shape and size.

key problems and laboratory investigations. Here we have described a progression of computational investigations which began with the calculations by Wang and Brennen (40,41,42) of the behaviour of a spherical cloud of bubbles subjected to a low pressure episode. Wang and Brennen (50) then extended this one-dimensional methodology to investigate the steady flow of a bubbly, cavitating mixture through a convergent/divergent nozzle. Under certain parametric conditions, the results are seen to model the dynamics of flashing within the nozzle. Moreover, it is clear from these steady flow studies that there are certain conditions in which no steady state solution exists and it is speculated that the flow under those conditions may be inherently unstable. Of course, it has frequently been experimentally observed that cavitating nozzle flows can become unstable and oscillate violently. Finally, we have also described recent efforts (Colonus *et al.* (46)) to extend the code to two and three space dimensions.

In conclusion, these recent investigations provide new insights into the dynamics and acoustics both of individual cavitation bubbles and of clouds of bubbles. In turn, these insights suggest new ways of modifying and possibly ameliorating cavitation noise and damage.

10. Acknowledgements

Our profound thanks to the Office of Naval Research for the support which it provided under contract N00014-97-1-0002 and to the technical monitor Edwin Rood who sponsored much of the research described herein.

REFERENCES

1. Reisman, G.E., Wang, Y.-C. and Brennen, C.E., "Observations of shock waves in cloud cavitation," *J. Fluid Mech.*, 1998, Vol. 355, pp. 255-283.
2. Mørch, K.A., "On the collapse of cavity cluster in flow cavitation," *Proc. First Int. Conf. on Cavitation and Inhomogenities in Underwater Acoustics, Springer Series in Electrophysics*, 1980, Vol. 4, pp. 95-100.
3. Mørch, K.A., "Cavity cluster dynamics and cavitation erosion," *Proc. ASME Cavitation and Polyphase Flow Forum*, 1981, pp. 1-10.
4. Hanson, I., Kedrinskii, V.K. and Mørch, K.A., "On the dynamics of cavity clusters," *J. Appl. Phys.*, 1981, Vol. 15, pp. 1725-1734.
5. Knapp, R.T., "Recent investigation on the mechanics of cavitation and erosion damage," *Trans. ASME*, 1955, pp. 1045-1054.
6. Bark, G. and van Berlekom, W.B., "Experimental investigations of cavitation noise," *Proc. 12th ONR Symp. on Naval Hydrodynamics*, 1978, pp. 470-493.
7. Soyama, H., Kato, H. and Oba, R., "Cavitation observations of severely erosive vortex cavitation arising in a centrifugal pump," *Proc. Third I.Mech.E. Int. Conf. on Cavitation*, 1992, pp. 103-110.
8. Wade, R.B. and Acosta, A.J., "Experimental observations on the flow past a plano-convex hydrofoil," *ASME J. Basic Eng.*, 1966, Vol.88, pp. 273-283.

9. Shen, Y. and Peterson, F.B., "Unsteady cavitation on an oscillating hydrofoil," *Proc. 12th ONR Symp. on Naval Hydrodynamics*, 1978, pp. 362-384.
10. Shen, Y. and Peterson, F.B., "The influence of hydrofoil oscillation on boundary layer transition and cavitation noise," *Proc. 13th ONR Symp. on Naval Hydrodynamics*, 1980, pp. 221-241.
11. Bark, G., "Developments of distortions in sheet cavitation on hydrofoils," *Proc. ASME Int. Symp. on Jets and Cavities*, 1985, pp. 215-225.
12. Franc, J.P. and Michel, J.M., "Unsteady attached cavitation on an oscillating hydrofoil," *J. Fluid Mech.*, 1988, Vol. 193, pp. 171-189.
13. Hart, D.P., Brennen, C.E. and Acosta, A.J., "Observations of cavitation on a three dimensional oscillating hydrofoil," *ASME Cavitation and Multiphase Flow Forum*, 1990, FED-Vol.98, pp. 49-52.
14. Kubota, A., Kato, H., Yamaguchi, H. and Maeda, M., "Unsteady structure measurement of cloud cavitation on a foil section using conditional sampling," *ASME J. Fluids Eng.*, 1989, Vol. 111, pp. 204-210.
15. Kubota, A., Kato, H. and Yamaguchi, H., "A new modelling of cavitating flows - a numerical study of unsteady cavitation on a hydrofoil section," *J. Fluid Mech.*, 1992, Vol. 240, pp. 59-96.
16. Le, Q., Franc, J.M. and Michel, J.M., "Partial cavities: global behaviour and mean pressure distribution," *ASME J. Fluids Eng.*, 1993, Vol. 115, pp. 243-248.
17. de Lange, D.F., de Bruin, G.J. and van Wijngaarden, L., "On the mechanism of cloud cavitation - experiment and modelling," *Proc. 2nd Int. Symp. on Cavitation, Tokyo*, 1994, pp. 45-49.
18. Kawanami, Y., Kato, H., Yamaguchi, H., Tagaya, Y. and Tanimura, M., "Mechanism and control of cloud cavitation," *Proc. ASME Symp. on Cavitation and Gas-Liquid Flows in Fluid Machinery and Devices*, 1996, FED-Vol.236, pp. 329-336.
19. McKenney, E.A. and Brennen, C.E., "On the dynamics and acoustics of cloud cavitation on an oscillating hydrofoil", *Proc. ASME Symp. on Cavitation and Gas-Liquid Flows in Fluid Machinery and Devices*, 1994, FED-Vol.190, pp. 195-202.
20. Reisman, G.E., McKenney, E.A. and Brennen, C.E., "Cloud cavitation on an oscillating hydrofoil," *Proc. 20th ONR Symp. on Naval Hydrodynamics*, 1994, pp. 78-89.
21. Morgan, W.B., personal communication, 1995.
22. Ukon, Y., "Cavitation characteristics of a finite swept wing and cavitation noise reduction due to air injection," *Proc. Int. Symp. on Propeller and Cavitation*, 1986, pp. 383-390.
23. Arndt, R.E.A., Ellis, C.R. and Paul, S., "Preliminary investigation of the use of air injection to mitigate cavitation erosion," *Proc. ASME Symp. on Bubble Noise and Cavitation Erosion in Fluid Systems*, 1993, FED-Vol.176, pp. 105-116.
24. Reisman, G.E. and Brennen, C.E., "Shock wave measurements in cloud cavitation," *Proc. 21st Int. Symp. on Shock Waves*, 1997, Paper 1570.
25. Reisman, G.E., Duttweiler, M.E. and Brennen, C.E., "Effect of air injection on the cloud cavitation of a hydrofoil," *Proc. ASME Fluids Eng. Div. Summer Meeting*, 1997, Paper No. FEDSM97-3249.
26. van Wijngaarden, L., "On the collective collapse of a large number of gas bubbles in water," *Proc. 11th Int. Conf. Appl. Mech.*, Springer-Verlag, Berlin, 1964, pp. 854-861.
27. Brennen, C.E., "Cavitation and bubble dynamics," 1995, Oxford University Press.
28. Chahine, G.L. "Cloud cavitation theory," *Proc. 14th ONR Symp. on Naval Hydrodynamics*, 1982, p. 51.
29. Noordij, L. and van Wijngaarden, L., "Relaxation effects, caused by relative motion, on shock waves in gas-bubble/liquid mixtures," *J. Fluid Mech.*, 1974, Vol. 66, pp. 115-143.

30. Kameda, M. and Matsumoto, Y., "Structure of shock waves in a liquid containing gas bubbles," *Proc. IUTAM Symp. on Waves in Liquid/Gas and Liquid/Vapour Two-Phase Systems*, 1995, pp. 117-126.
31. d'Agostino, L. and Brennen, C.E., "On the acoustical dynamics of bubble clouds," *ASME Cavitation and Multiphase Flow Forum*, 1983, pp. 72-75.
32. d'Agostino, L. and Brennen, C.E., "Acoustical absorption and scattering cross-sections of spherical bubble clouds," *J. Acoust. Soc. of Amer.*, 1988, Vol. 84, No.6, pp. 2126-2134.
33. d'Agostino, L. and Brennen, C.E., "Linearized dynamics of spherical bubble clouds," *J. Fluid Mech.*, 1989, Vol. 199, pp. 155-176.
34. Omta, R., "Oscillations of a cloud of bubbles of small and not so small amplitude," *J. Acoust. Soc. Am.*, 1987, Vol. 82, pp. 1018-1033.
35. Prosperetti, A., "Bubble-related ambient noise in the ocean," *J. Acoust. Soc. Am.*, 1988, Vol. 84, pp. 1042-1054.
36. Kumar, S. and Brennen, C.E., "Non-linear effects in the dynamics of clouds of bubbles," *J. Acoust. Soc. Am.*, 1991, Vol. 89, pp. 707-714.
37. Kumar, S. and Brennen, C.E., "Harmonic cascading in bubble clouds," *Proc. Int. Symp. on Propulsors and Cavitation, Hamburg*, 1992, pp. 171-179.
38. Kumar, S. and Brennen, C.E., "Some non-linear interactive effects in bubbly cavitating clouds," *J. Fluid Mech.*, 1993, Vol. 253, pp. 565-591.
39. Chahine, G.L. and Duraiswami, R., "Dynamical interactions in a multibubble cloud," *ASME J. Fluids Eng.*, 1992, Vol. 114, pp. 680-686.
40. Wang, Y.-C. and Brennen, C.E., "Shock wave development in the collapse of a cloud of bubbles," *ASME Cavitation and Multiphase Flow Forum*, 1994.
41. Wang, Y.-C. and Brennen, C.E., "The noise generated by the collapse of a cloud of cavitation bubbles," *ASME Symp. on Cavitation and Gas-Liquid Flows in Fluid Machinery and Devices*, 1995, FED-Vol. 226, pp. 17-29.
42. Wang, Y.-C. and Brennen, C.E., "Shock wave and noise in the collapse of a cloud of cavitation bubbles," *Proc. 20th Int. Symp. on Shock Waves, Pasadena*, 1995, pp. 1213-1218.
43. Wang, Y.-C., "Effects of nuclei size distribution on the dynamics of a spherical cloud of cavitation bubbles," *Proc. ASME Fluids Eng. Div. Summer Meeting, Washington, D.C.*, 1998.
44. Mellen, R.H., "Ultrasonic spectrum of cavitation noise in water," *J. Acoust. Soc. Am.*, 1954, Vol. 26, No.3, pp. 356-360.
45. Blake, W. K., Wolpert, M. J. and Geib, F. E., "Cavitation noise and inception as influenced by boundary-layer development on a hydrofoil," *J. Fluid Mech.*, 1977, Vol. 80, pp. 617-640.
46. Colonius, T., Brennen, C.E. and d'Auria, F., "Computation of shock waves in cavitating flows," *Proc. ASME Fluids Eng. Div. Summer Meeting, Washington, D.C.*, 1998.
47. Brennen, C.E., Colonius, T., d'Auria, F. and Preston, A., "Computing shock waves in cloud cavitation," *Proc. CAV98 Third Int. Symp. on Cavitation, Grenoble, France*, 1998.
48. Smereka, P. and Banerjee, S., "The dynamics of periodically driven bubble clouds," *Phys. Fluids*, 1988, Vol. 31, pp. 3519-3531.
49. Lauterborn, W. and Koch, A., "Holographic observation of period-doubled and chaotic bubble oscillations in acoustic cavitation," *Phys. Rev. A*, 1987, Vol. 35, No.4, pp. 1974-1976.
50. Wang, Y.-C. and Brennen, C.E., "One-dimensional bubbly cavitating flows through a converging-diverging nozzle," *ASME J. Fluids Eng.*, 1998, Vol. 120, pp. 166-170.
51. Chapman, R.B. and Plesset, M.S., "Thermal effects in the free oscillation of gas bubbles," *ASME J. Basic Eng.*, 1971, Vol. 93, pp. 373-376.
52. Song, C.S., "Direct numerical simulation of sheet cavitation and cloud cavitation," *Presentation to 1997 ONR Workshop on the Dynamics of Bubbly Flows, San Diego*.

53. Merkle, C. and Feng, J., "Dynamics of sheet cavitation," *Presentation to 1998 ONR Workshop on Free Surface Turbulence and Bubbly Flows, Pasadena, CA.*
54. Sturtevant, B. and Kulkarny, V.J., "The focusing of weak shock waves," *J. Fluid Mech.*, 1996, Vol. 73, pp. 651-680.
55. Blake, W.K., "*Mechanics of flow-induced sound and vibration*", 1986, Academic Press, New York.
56. Blake, W.K., "Propeller cavitation noise. The problems of scaling and prediction," *Proc. Int. ASME Symp. on Cavitation and Multiphase Flow Noise*, 1986, pp. 89-99.
57. Sturtevant, B. and Kulkarny, V.J., "The focusing of weak shock waves," *J. Fluid Mech.*, 1996, Vol. 73, pp. 651-680.

DISCUSSION

J. Duncan
University of Maryland, USA

The authors are to be commended for elucidating a number of interesting dynamic effects with a relatively simple model. How would you expect your spherical cloud results to change if you included liquid compressibility in the calculations? Of particular interest to me are the effects of shocks, created by collapsing bubbles, on neighboring bubbles.

AUTHORS' REPLY

I thank Professor Duncan for his kind remarks. In response to his question, the liquid compressibility plays a quite minor role in the mechanics since the bubble "compressibility" is so much greater. In past analysis (see d'Agostino and Brennen, *JFM*, 1989, Vol. 199, pp. 155-176) we have included this effect for completeness and demonstrated the effect to be small. In the present analyses it was omitted for simplicity.